13th World Conference on Earthquake Engineering
Vancouver, B.C., Canada
August 1-6, 2004
Paper No. 688

DEVELOPMENT OF THE INELASTIC DEMAND SPECTRA CONSIDERING HYSTERETIC CHARACTERISTICS AND SOIL CONDITIONS

Hyun-Ho LEE[1], Kee-Tae HWANG[2]

SUMMARY

The inelastic demand caused by earthquake load is strongly related to the natural period, displacement ductility ratio, hysteretic characteristics of structures and soil conditions. The objective of this study is a determination method proposition for the inelastic demand of earthquake hazards for the using in capacity spectrum method. Five different hysteretic models are used which are elasto-perfectly plastic, bilinear, strength deterioration, stiffness degradation and pinching models. For a given target ductility ratio, inelastic demand is evaluated by using nonlinear time-history analysis with recorded earthquake ground motions for three types of soil condition. Used earthquake records were selected by calibration parameters of PGA, PGV, EPA and EPV. To determine the ductility factor of rock site, regression analysis is used by ductility factor and period characteristics of elasto- perfectly plastic response. By two-stage analysis, a functional equation for the inelastic demand spectra was derived from ductility factor and hysteretic characteristics. By the same procedure of rock site, functional equations for stiff and soft soil sites were also derived. From the compatibility analysis and statistical studies of nonlinear time-history analysis, developed method of the inelastic demand in capacity spectrum can be used to find the performance point in seismic performance of structures.

INTRODUCTION

In most seismic provisions, structural safety to the earthquake has been evaluated by story drift ratio that is calculated by displacement response, whereas design earthquake load is represented by acceleration spectrum. Therefore, it is useful way that strength demand and displacement demand represent in one demand spectrum. In performance based seismic design as FEMA 273, 368 [1,2] building performance level is considered by the inelastic behavior such as life safety and collapse prevention level. The determination method of inelastic demand spectrum (IDS) is needed for the inelastic performance evaluation of structures. And the hysteretic effects in capacity spectrum method (CSM) might be reflected to demand spectrum. Because capacity spectrum is evaluated by simple nonlinear static analysis.

[1] Professor, Dept. of Architectural Eng., Dong Yang University, Korea. Email:hhlee@phenix.dyu.ac.kr
[2] Principal Engineer, Archineering Corporation, Korea. Email:hwanakt21@naver.com

Moreover, this can not represent the hysteretic behaviors such as strength deterioration, stiffness degradation and pinching effect.
The inelastic demand caused by earthquake load is deeply related to the elastic demand with natural period, displacement ductility ratio and variety of hysteretic behaviors. The hysteretic characteristics that affect to the structural behaviors are classified by elasto-perfectly plastic, bilinear, strength deterioration, stiffness degradation and pinching model. The elasto-perfectly plastic model is idealized as zero second slopes. Bilinear model has a second slope to represent the post-yield stiffness. Strength deterioration and stiffness degradation models represent the decreasing strength and decreasing stiffness, respectively. Pinching model represents the crack open-closure movement of concrete.
The seismic evaluation result of a four-story reinforced concrete building by Kunnath, Mattox and Reinhorn (1996) [3] is shown in Fig. 1. To determine the response for five earthquake motion intensities, they used nonlinear time-history analysis, as well as simplified elastic and inelastic response evaluation method. By using a bilinear model, the spectral curves were generated for the inelastic response evaluation. The response of the building was obtained for a give value of second slope, i.e. post-yield stiffness. To define the different stage of the yield strength, force reduction factor (R), which is the ratio of the inelastic yield force (V_y) to the elastic yield force (V_e), was used. Eq. (1) shows the ductility ratio as R factor.

$$R = \frac{V_e}{V_y} \tag{1}$$

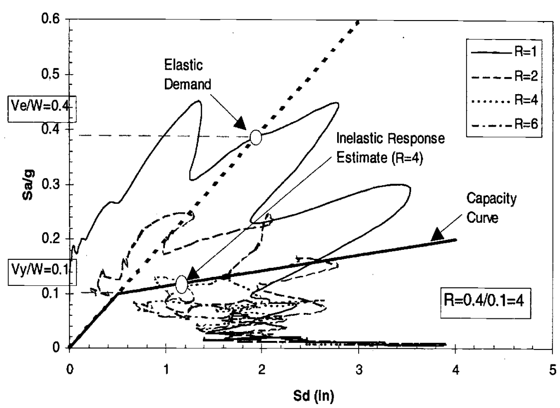

Fig. 1 Using capacity spectrum method by Kunnath et.al. (1996).

As shown in Fig. 1, it is very difficult to find the performance point because of the ambiguous shape of demand spectrum at a high level of reduction factor, i.e. R=6. Therefore, the determination method, which evaluates the inelastic demand for given target ratio with generalized earthquake responses, should be considered.
The objective of this study is a determination method proposition for the inelastic demand of earthquake hazards in CSM. To achieve the goal, five different hysteretic models and three soil types are used. Using models are elastic perfectly plastic (EPP), bilinear, strength deterioration, stiffness degradation and pinching model. Using soil types are S_1, S_2, S_3. The IDS are obtained from a given target ductility ratio. For a given target ductility ratio, IDS can be obtained by using nonlinear time-history analysis of single degree of system with selected earthquake records. The effect of each hysteretic model under demand spectrum is investigated by comparing the demand spectrum of each hysteretic model with that of EPP model. To determine the ductility factor, regression analysis is applied by ductility factor and period characteristics of EPP response. Based on the ductility factor for EPP model, a functional equation can be derived from ductility factor and hysteretic characteristics by two-stage analysis.

METHOD OF INELASTIC DEMAND EVALUATION

Estimation procedure of inelastic demand spectrum

As shown in Eq. (2), elastic displacement response (S_d) is estimated by a period (T) and an elastic acceleration response (S_a). Inelastic acceleration response (S_{ain}) is estimated by elastic acceleration response and ductility factor (R_μ) in Eq. (3). The ductility factor is derived from many researching groups such as Newmark and Hall (1982) [4], Krawinkler and Nassar (1992) [5], Miranda and Bertero (1994) [6] and Lee et al. (1999) [7]. Where ductility factor is defined as the ratio of the inelastic demand to the elastic demand, and is consisted by a function of period (T), displacement ductility ratio (μ) and hysteretic characteristics (α) as shown in Eq. (4). From the Eq. (2) and Eq. (3), the inelastic displacement demand is derived as shown in Eq. (5). In Eq. (5), displacement ductility ratio is used to estimate the maximum inelastic displacement response.

$$S_d = \frac{T^2}{4\pi^2} \times S_a \tag{2}$$

$$S_{ain} = \frac{S_a}{R_\mu} \tag{3}$$

$$R_\mu = f(T, \mu, \alpha) \tag{4}$$

$$S_{din} = \frac{T^2}{4\pi^2} \times S_{ain} \times \mu \tag{5}$$

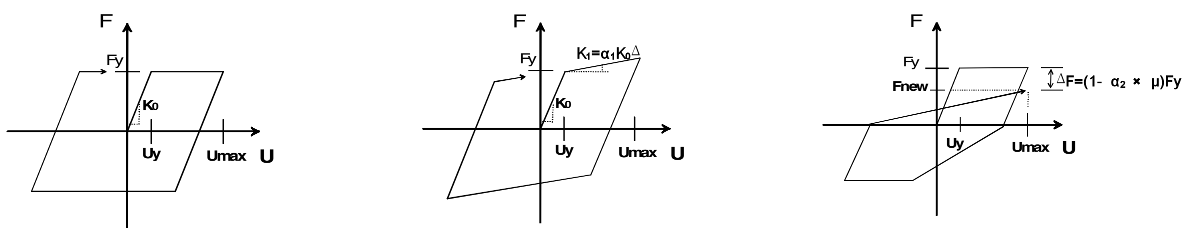

(a) Elasto perfectly plastic (b) Binear (c) Strength deterioration

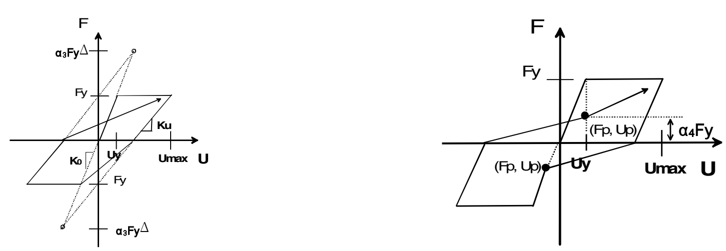

(d) Stiffness degradation (e) Pinching.

Fig. 2 Used hysteretic model.

The inelastic demand caused by earthquake hazard is estimated by lateral yield strength of single degree of system according to displacement ductility ratio. The inelastic lateral yield strength (F_y) is estimated by repeating procedure of decreasing ductility ratio to the target ductility ratio. In addition, the inelastic responses are evaluated by nonlinear time history analysis of 5 % damped single degree of system. Using the Eq. (2) ~ Eq. (5), IDS can be determined. To consider the different hysteretic effect such as elasto-perfectly plastic, bilinear, strength deterioration, stiffness degradation and pinching, same procedure is adopted which is used in the study of Lee et al. (1999) [7]. Each hysteretic characteristic is derived from following conditions.

- The influence of natural period, which affect to the inelastic response is estimated by an EPP model according to displacement ductility ratio.
- Each coefficient of hysteretic models is estimated by displacement ductility ratio and hysteretic characteristics.

Where the analyzing parameters and shapes of each hysteretic model are listed in Fig. 2.

Used earthquake records

The linear elastic design response spectrum (LEDRS) that is represented by a design earthquake load is not necessarily the ideal means for describing the earthquake ground motion (EQGM) because it does not contain enough information about the EQGM such as duration, characteristics of the site and inelastic demand for structures. In buildings that have severe irregularity, long natural periods and historical values, the use of EQGM records as input design loads is more desirable than using LEDRS. ATC 3-06 [8] recommends using a set of four or more EQGM records whose average elastic response spectrum is similar to the LEDRS in the seismic code.

The scaling parameters, generally, to calibrate the EQGMs that fit the target LEDRS in design code are peak ground acceleration (PGA), peak ground velocity (PGV), effective peak acceleration (EPA) and effective peak velocity (EPV). The EPA and EPV are defined by Eq. according to ATC 3-06.

$$EPA = \frac{S_a}{2.5} \quad EPV = \frac{S_v}{2.5} \tag{6}$$

Where S_a and S_v denote an average spectral acceleration in the period range 0.1 to 0.5 second and an average spectral acceleration of about 1 second, respectively.

The EQGM records used in this study were selected from the earthquake strong motion CD-ROM by the United States Department of Commerce (1996) [9] and the U. S. Geological Survey digital data series DDS-7 CD-ROM (1992) [10]. Basic strong motion acceleration processing software (BAP) [11] was used for correcting the EQGM records from the CD-ROM. The LEDRS in Ministry of Construction & Transportation in Korea (MCT 97) was used as a target response spectrum which was proposing the seismic hazard coefficients obtained from the probabilistic studies of historical and recorded ground motions at 1997 by Ministry of Construction & Transportation in Korea. To calibrate the EQGM records so that their responses fit the target LEDRS, an acceleration response and a velocity response must be considered. Therefore two sets of calibration parameters are considered. One is a characteristic of ground shaking such as PGA and PGV, and the other is a characteristic of response such as EPA and EPV. Following this procedure, the finally selected EQGM responses by a PGA are shown in Fig. 3. Finally, 77 EQGM records are selected for the using of inelastic demand evaluation.

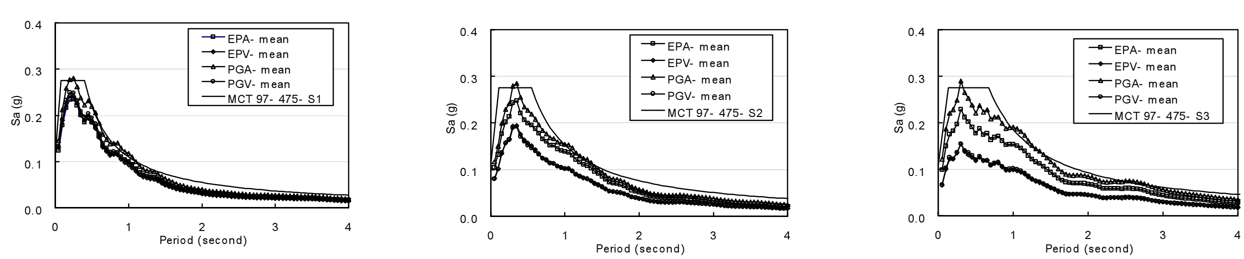

(a) S_1 soil site (b) S_2 soil site (c) S_3 soil site.

Fig. 3 Selected EQGM records by PGA.

DUCTILITY FACTOR DETERMINATION OF ELASTO-PERFECTLY PLASTIC MODEL

Compatibility evaluation of ductility factor and inelastic displacement response

The inelastic demand of elasto-perfectly plastic (EPP) model is estimated by ductility factor (R_μ) that is evaluated by reducing lateral yield strength to the target ductility ratio. Where the ratio of 1 (elastic), 2, 4 and 6 mean the level of target ductility ratio. To analyze the compatibility of this study results, proposed method of ductility factor by Newmark and Hall (1982) [4], Krawinkler and Nassar (1992) [5], Miranda and Vertero (1994) [6], Lee et al. (1999) [7] are considered. Detailed equations of ductility factor estimation are as follows;

● Newmark and Hall (1982)

$$R_\mu = 1.0 \qquad (T \le 0.03 \text{ second}) \tag{7}$$

$$R_\mu = \sqrt{2\mu - 1} \qquad (0.12 \le T \le 0.5 \text{ second})$$

$$R_\mu = \mu \qquad (1.0 \le T \text{ second})$$

where, μ : ductility ratio

● Krawinkler and Nassar (1992)

$$R_\mu = [c(\mu - 1) + 1]^{1/c} \tag{8}$$

$$c(T, \alpha) = \frac{T^a}{1 + T^a} + \frac{b}{T}$$

where, α : post yield stiffness (%)

α = 0% : a=1.0, b=0.42 (EPP model)

α = 2% : a=1.0, b=0.37

α =10% : a=1.0, b=0.29

● Miranda and Vertero (1994)

$$R_\mu = \frac{\mu - 1}{\phi} + 1 \tag{9}$$

where, $\phi = 1 + \frac{1}{10T - \mu T} - \frac{1}{2T} e^{-1.5(in(T) - 0.6)^2}$, for rock site (S_1 soil site)

$\phi = 1 + \frac{1}{12T - \mu T} - \frac{2}{5T} e^{-2(in(T) - 0.2)^2}$, for alluvium site (S_2 soil site)

$\phi = 1 + \frac{T_g}{3T} - \frac{3T_g}{4T} e^{-3(in(T/T_g) - 0.25)^2}$, for soft site (S_3 soil site)

T_g : predominent period of ground

● Lee, Han and Oh (1999)

$$R_\mu = A_0 \times \{1 - \exp(-B_0 \times T)\} \tag{10}$$

where, $A_0 = 0.99 \times \mu + 0.15$

$B_0 = 23.69 \times \mu^{-0.83}$

From the proposed ductility factor evaluation method through Eq. (7) to Eq. (10), estimated results and this study results are shown in Fig. 4. Where target ductility ratio is 6 and soil condition is rock site (S_1). In Fig. 4, results of this study are evaluated as similar to the proposed method. To review the data dispersion of each ductility ratio, coefficient of variation (COV) in Table 1 is used for the results of this study, Miranda (1991) [13], and Lee et al. (1999). The meaning of COV is defined as the ratio of mean value to standard deviation of data. From this, this study is very similar to the other studies. From Fig. 4 and Table 1, the results of this study have been proofed as adequate.

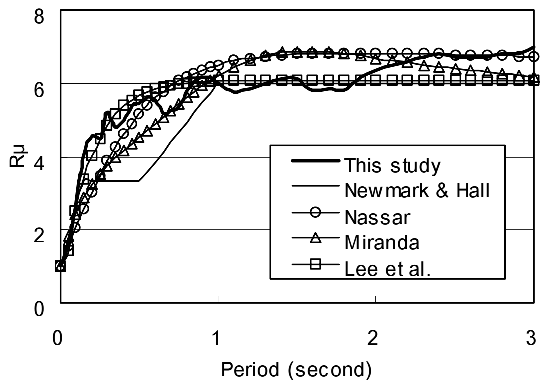

Fig. 4 Comparison of ductility factor (μ=6, S_1).

Table 1 Ductility factor comparison by coefficient of variable.

Researcher	μ =2	μ =4	μ =6
This study	0.23	0.35	0.40
Miranda	0.25	0.35	0.40
Lee et al.	0.23	0.33	0.39

To proof the compatibility of displacement response, the ratio of inelastic displacement response over elastic response is used. Where, the inelastic displacement demand can be estimated by the ductility factor according to each period range. Fig. 5 shows the displacement response ratio with the results of this study, Miranda (1991) and Krawinkler (1992). The meaning of μ/R_μ in Fig. 5 (c) is same as the ratio of elastic to inelastic responses. As shown in Fig. 5, the result of this study is very similar to the results of Miranda and Krawinkler. From this, estimated results of inelastic displacement are evaluated as adequate.

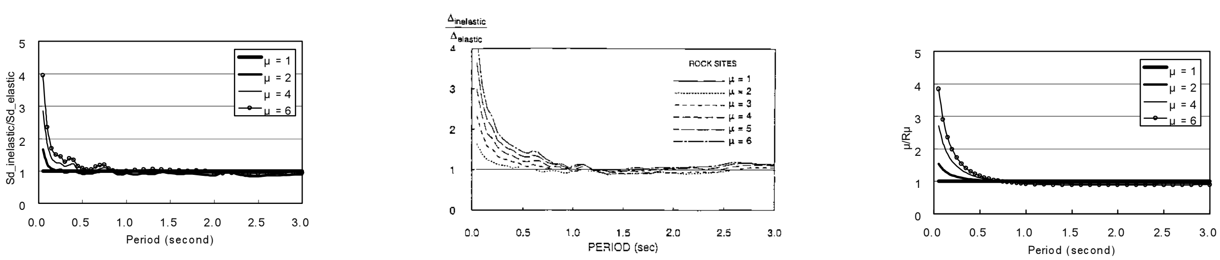

(a) This study (b) Miranda (c) Krawinkler

Fig. 5 Comparison of inelastic displacement response.

After the examination of ductility factor and inelastic response, inelastic demand of EPP model according to natural period can be estimated by acceleration response (S_a) and displacement response (S_d). Fig. 6 (a), (b) shows the acceleration response and displacement response according to ductility ratio in natural period range. IDS, which is consisted by S_a and S_d is shown in Fig. 6 (c). In Fig. 6 (a), the amount of inelastic S_a is distinctively reduced than elastic S_a (μ=1). Over the ductility ratio 4, amount of inelastic S_a is shown as similar in spite of ductility level increase. The inelastic S_d in Fig. 6 (b) is evaluated as similar in spite of the ductility level increase as shown in the results of Miranda and Krawinkler in Fig 5. The IDS in Fig. 6 (c) is strongly affected by S_a which governed the IDS shape. And IDS is affected by ductility ratio.

Consequently IDS was deeply related to the S_a and IDS can be estimate by S_a because S_d dos not have the incremental values according to the ductility level increase.

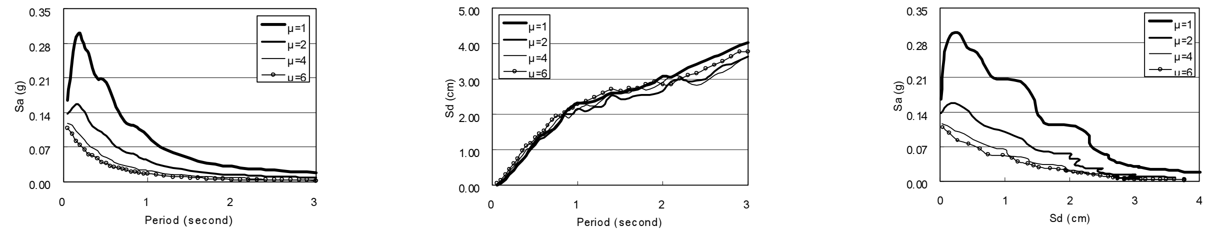

(a) Acceleration response (b) Displacement response (c) Inelastic demand spectrum

Fig. 6 Inelastic response of EPP model.

Proposition of ductility factor for the EPP model

Even if there are many ductility factor evaluation methods for the EPP model, it is the best way to modify or suggest an evaluation method that is making a convenient form for the user with the accuracy. Based on the research results of Lee et al. (1999) [7], the equation of ductility factor (R_μ) for the EPP model is modified with the nonlinear time-history analysis of EQGM records for S_1 soil site. The response of EPP model is consisted by ductility factor (R_μ), ductility ratio (μ) in natural period (T) range. To decouple the effect of ductility ratio and natural period in ductility factor, two-stage regression analysis is considered. In the first stage, ductility factor is regressed by the each ductility ratio in each period range. The regression result of ductility factor is shown in Fig. 7. And these are shown the coefficients of a and b in the structure of R_μ functions. To analyze ductility factor and the coefficients, the results of second stage regression analysis is shown in Fig. 8. In using of ductility ratio and natural period, a functional form of ductility factor for the EPP model in S_1 soil site is derived as shown in Eq. (11)

$$R_\mu = A_0 \times \{1 - \exp(-B_0 \times T)\} \tag{11}$$

where, $A_0 = 1.03\mu^{1.04}$

$B_0 = 27.42\mu^{-0.86}$

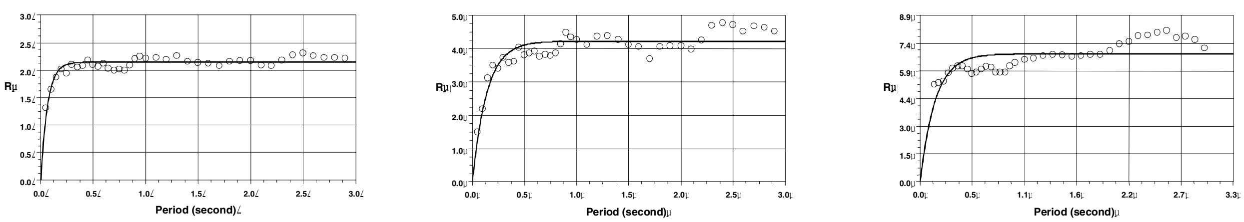

(a) μ=2 (b) μ=4 (c) μ=6

Fig. 7 First stage regression analysis of R_μ for the EPP model.

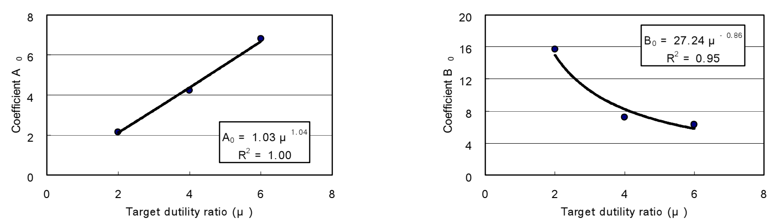

(a) Coefficient A_0 (b) Coefficient B_0.

Fig. 8 Second stage regression analysis of R_μ for the EPP model.

To estimate the coefficients of ductility factor in S_2 and S_3 soil sites, same procedure for S_1 site is also used. From this, Eq. (11) is modified as Eq. (12) with the coefficients a_1, a_2, b_1, b_2, which is listed in Table 2.

$$R_\mu = A_0 \times \{1 - \exp(-B_0 \times T)\} \tag{12}$$

where, $A_0 = a_1 \mu^{a_2}$

$B_0 = b_1 \mu^{-b_2}$

Table 2 Soil type coefficients.

Coefficient	S_1	S_2	S_3
a_1	1.03	1.04	1.01
a_2	1.04	0.98	1.03
b_1	27.24	17.36	23.01
b_2	0.86	0.90	1.24

INELASTIC DEMAND EVALUATION OF HYSTERETIC MODELS

Calibration factor for the bilinear model

The calibration factors for the hysteretic effects are evaluated as the same procedure of that of EPP model done. Characteristic parameter of hysteretic model and ductility ratio are considered by the two-stage analysis. From the previous research of Krawinkler and Nassar (1992) and Lee et al. (1999), the bilinear model that consider the post-yield stiffness as second slope should has been decreasing the inelastic demand or input earthquake demand. The characteristic parameter of the bilinear model is symbolized as α_1, which means the ratio of post-yield stiffness as in Fig. 2 (b). The calibration factor for the bilinear model is also symbolized as $C_{\alpha 1}$ and it is multiplied to the ductility factor of EPP model in Eq. (11). In the evaluation procedure for the bilinear model, considered post-yield stiffness ratios (α_1) are 0.02, 0.05 and 0.10. Where the meaning of $\alpha_1 = 0$ is a response of EPP model. Table 3 shows the ductility factor ratio of the bilinear model to that of EPP model in given ductility ratio. Where the ratio is evaluated by the mean value of each EQGM records and natural period. From this, the increasing of post-yield stiffness and ductility ratio can be making the decreasing of the inelastic demand. Therefore calibration factor ($C_{\alpha 1}$) for the bilinear model will be derive in consideration of post-yield stiffness ratio (α_1) and ductility ratio (μ). To decouple the effect of α_1 and μ, two-stage regression analysis is considered. In the first stage, α_1 is regressed by the each ductility ratio in each period range. To analyze the coefficients A_1 and B_1, the second stage regression analysis is applied. In using of α_1 and coefficients, a functional form of $C_{\alpha 1}$ for the bilinear model is derived as shown in Eq. (13).

$$C_{\alpha 1} = A_1 \times \alpha_1^{-B1} \tag{13}$$

where, $A_1 = 0.99 \mu^{-0.2}$

$B_1 = 0.02 \mu^{0.8}$

Table 3 Ductility factor ratio for the bilinear model.

Post yield stiffness ratio	$\alpha_1 = 0.02$	$\alpha_1 = 0.05$	$\alpha_1 = 0.10$
$\mu = 2$	0.980	0.957	0.931
$\mu = 4$	0.945	0.897	0.856
$\mu = 6$	0.919	0.862	0.823

Calibration factor for the strength deterioration model

When structure or member has weak shear capacity than the applied shear force, the strength deterioration of system is considered. This phenomenon is shown after the experience of yielding. The characteristic parameter of the strength deterioration model is symbolized as α_2, which means decreasing ratio of yield strength of a system as in Fig. 2 (c). The calibration factor for the strength deterioration model is also symbolized as $C_{\alpha2}$ and it is multiplied to the ductility factor of EPP model in Eq. (11) as the same procedure of bilinear model. In the evaluation procedure for this model, considered strength deterioration ratios (α_2) are 0.05, 0.10 and 0.20. Where the meaning of α_2 =0 is a response of EPP model. Table 4 shows the ductility factor ratio of the strength deterioration model to that of EPP model in given ductility ratio. Where the ratio is evaluated by the mean value of each EQGM records and natural period. From the Table 4, the increasing of strength deterioration and ductility ratio can be making an increasing of the inelastic demand. Therefore calibration factor ($C_{\alpha2}$) for the strength deterioration model will be derive in consideration of α_2 and μ. To decouple the effect of α_2 and μ, two-stage regression analysis is considered. In the first stage, α_2 is regressed by the each ductility ratio in each period range. To analyze the coefficients A_2 and B_2, the regression analysis of second stage is applied. In using of α_2 and coefficients, a functional form of $C_{\alpha2}$ for the strength deterioration model is derived as shown in Eq. (14).

$$C_{\alpha 2} = A_2 \times \alpha_2^{B2} \tag{14}$$

where, $A_2 = 1.23 \times \exp(0.04\mu)$

$B_2 = 0.06 \times \exp(0.04\mu)$

Table 4 Ductility factor ratio for the strength deterioration model.

Strength deterioration ratio	α_2 =0.05	α_2 =0.10	α_2 =0.20
μ =2	1.115	1.163	1.214
μ =4	1.180	1.232	1.299
μ =6	1.261	1.340	1.399

Calibration factor for the stiffness degradation model

Among the shear governed hysteretic behavior, the stiffness degradation could be reduced energy dissipation capacity of structures, which increases the inelastic demand. The characteristic parameter of the stiffness degradation model is symbolized as α_3, which means the ratio of stiffness degradation of a system as in Fig. 2 (d). The calibration factor for the stiffness degradation model is also symbolized as $C_{\alpha3}$ and it is multiplied to the ductility factor in Eq. (11) as the same procedure of strength deterioration model. In the evaluation procedure for this model, considered stiffness degradation ratios (α_3) are 3, 1 and 0 Where α_3 =15 is a response of EPP model. Table 5 shows the ductility factor ratio of the stiffness degradation model to that of EPP model in given ductility ratio. From the Table 5, the increasing of stiffness degradation and ductility ratio can be making an increasing of the inelastic demand. Therefore calibration factor ($C_{\alpha3}$) for the stiffness degradation model will be derive in consideration of α_3 and μ. To analyze the effect of α_3 and μ, two-stage regression analysis is also considered. In the first stage, α_3 is regressed by the each ductility ratio in each period range. To analyze the coefficients A_3 and B_3, the regression analysis of second stage is applied. In using of α_3 and coefficients, a functional form of $C_{\alpha3}$ for the stiffness degradation model is derived as shown in Eq. (15).

$$C_{\alpha 3} = A_3 \times \exp(-B_3 \alpha_3) \tag{15}$$

where, $A_3 = 1.11\mu^{0.06}$

$B_3 = 0.04\mu^{0.22}$

Table 5 Ductility factor ratio for the stiffness degradation model.

Stiffness degradation ratio	α_3 =3	α_3 =1	α_3 =0
μ =2	1.043	1.081	1.187
μ =4	1.066	1.113	1.270
μ =6	1.083	1.134	1.271

Calibration factor for the pinching model

When the loading direction is reversed after the experience of yielding, opened-shear cracks of reinforced concrete member did not close due to shear. This phenomenon can make the distortion of the hysteretic loops, and it is called pinching effect. The pinching could be reduced energy dissipation capacity of structures, which increases the inelastic demand. The characteristic parameter of the pinching model is symbolized as α_4, which means the pinching ratio of a system as in Fig. 2 (e). The calibration factor for the pinching model is also symbolized as $C_{\alpha 4}$ and it is multiplied to the ductility factor in Eq. (11) as the same procedure of inelastic demand increasing model. In the evaluation procedure for this model, considered pinching ratios (α_4) are 0.7, 0.5 and 0.2 Where α_4 =1 is a response of EPP model. Table 6 shows the ductility factor ratio of the pinching model to that of EPP model in given ductility ratio. From the Table 6, the increasing of pinching and ductility ratio can be making an increasing of the inelastic demand. Therefore calibration factor ($C_{\alpha 4}$) for the pinching model will be derive in consideration of α_4 and μ. To analyze the effect of α_4 and μ, two-stage regression analysis is also considered. In the first stage, α_4 is regressed by the each ductility ratio in each period range. To analyze the coefficients A_4 and B_4, the regression analysis of second stage is applied. In using of α_4 and coefficients, a functional form of $C_{\alpha 4}$ for the pinching model is derived as shown in Eq. (16).

$$C_{\alpha 4} = A_4 \times \alpha_4^{-B4} \tag{16}$$

where, $A_4 = 1.12\mu^{0.02}$

$B_4 = 0.02\mu^{0.49}$

Table 6 Ductility factor ratio for the pinching model.

Pinching ratio	α_4 =0.7	α_4 =0.5	A_4 =0.2
μ =2	1.154	1.160	1.202
μ =4	1.173	1.195	1.248
μ =6	1.189	1.217	1.275

CONSTRUCTION OF INELASTIC DEMAND SPECTRUM

From the correlation evaluation between ductility ratio and coefficient of hysteretic characteristics, IDS can be made by the inelastic response with calibration factor by using the equation of Eq. (2) to Eq. (5). Calibration factor for the hysteretic models, which is based on the ratio to the response of EPP model, have been driven in such expression $C_{\alpha 1}$, $C_{\alpha 2}$, $C_{\alpha 3}$ and $C_{\alpha 4}$ to the bilinear, strength deterioration, stiffness degradation and pinching effect, respectively. Correlation factor in consideration of different hysteretic characteristics is multiplied to the ductility factor for the EPP model. Eq. (17) shows the finally proposed function for the ductility evaluation with calibration factors.

$$R_\mu = R(T,\mu) \times C_{\alpha 1} \times C_{\alpha 2} \times C_{\alpha 3} \times C_{\alpha 4} \tag{17}$$

where, $R(T,\mu)$: ductility factor of EPP model in Eq. (11and 12)

Fig. 9 shows the fitness of ductility factor in inelastic demand spectrum by Eq. (2), (3), (5) and (17). Where, the solid line represents the calculated ductility factor and dashed line represents the evaluated ductility factor. From this, calculated ductility factor can be well represents the evaluated results.

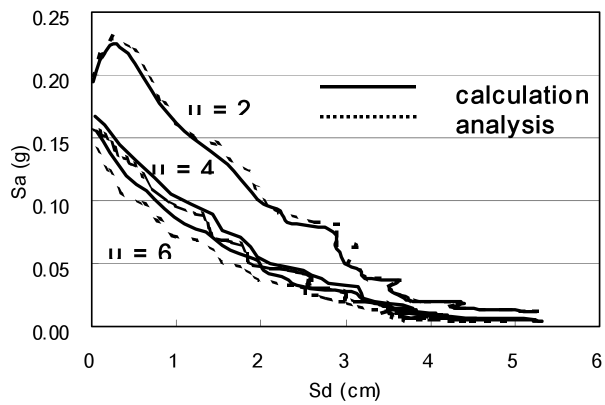

Fig. 9 Fitness of calculated IDS considering different hysteretic parameters (α_1=0.05, α_2=0.2, α_3=3, α_4=0.7).

CONCLUSIONS

The inelastic demand caused by earthquake load is deeply related to the elastic demand with natural period, displacement ductility ratio and variety of hysteretic behaviors. The hysteretic characteristics that affect to the behavior of structures are classified by elasto-perfectly plastic, bilinear, strength deterioration, stiffness degradation and pinching model. The objective of this study is a determination method proposition for the inelastic demand of earthquake hazards in capacity spectrum method. From the compatibility analysis and nonlinear time-history analysis, statistical studies are carried out to propose the ductility factor evaluation method with different hysteretic models and soil types. According to the results of this study, following conclusions are made:

1) Based on the research of Lee et al., equation of ductility factor (R_μ) for the EPP model is modified with the nonlinear time-history analysis of 77th EQGM records for soil types S_1, S_2 and S_3. The response of EPP model is consisted by ductility factor (R_μ), ductility ratio (μ) in natural period (T). By the two-stage regression analysis, a functional form of ductility factor for the EPP model is derived.

2) From the regression analysis, calibration factor ($C_{\alpha1}$, $C_{\alpha2}$, $C_{\alpha3}$ and $C_{\alpha4}$) for the bilinear, strength deterioration, stiffness degradation and pinching effect model is derived in consideration of hysteretic parameters and ductility ratio.

3) Consequentry, IDS is proposed in consideration of different hysteretic characteristics and soil types.

REFERENCES

1. Building Seismic Safety Council. "NEHRP guidelines for the seismic rehabilitation of buildings." Washington D. C: Building Seismic Safety Council for the Federal Emergency Management, Report No. FEMA 273, 1997.
2. Building Seismic Safety Council. "NEHRP recommended provisions for seismic regulations for new buildings." Washington D. C: Building Seismic Safety Council for the Federal Emergency

Management, Report No. FEMA 368, 2000.
3. Kunnath, S.K., Mattox, R.E.V., and Reinhorn, A.M. "Evaluation of sesmic damageability of a typical R/C building in midwest United States." Proceedings of 11th WCEE, Paper No. 1300, 1996.
4. Newmark N.M., and Hall, W.J. "Earthquake spectra and design. EERI." Berkeley, CA.: Earthquake Engineering Research Institute Monograph Series, 1982.
5. Krawinkler, H., and Nassar, A.A. "Seismic design based on ductility and cumulative damage demands and capacities." Elsevier Applied Science, 1992.
6. Miranda, E., and Bertero, V.V. "Evaluation of strength reduction factors for earthquake resistance design." Earthquake Spectra 1994; 10(2): 357-379.
7. Lee, L.H., Han, S.W., and Oh, Y.H. "Determination of ductility factor considering different hysteretic models." Earthquake Engineering and Structural Dynamics 1999; 28(9): 957-977.
8. Applied Technology Council. "Tentative provisions for the development of seismic regulations for buildings." Applied Technology Council, Report No. ATC 3-06, 2nd Printing, 1984.
9. United States Department of Commerce. "Earthquake strong motion. United States Department of Commerce." Colorado, 1996.
10. U. S. Geological Survey. "Earthquake strong motion. U. S. Geological Survey." 1992.
11. April M. Converse. "Basic strong-motion accelerogram processing software version 1.0 (BAP)." United States Department of the Interior U.S. Geological Survey, Open-File Report 92-296A, 1992.
12. International Conference of Building Officials. "Uniform building code." International Conference of Building Officials, Vol. 2, April 1997.
13. Miranda, E. "Seismic Evaluation and Upgrading of Existing Buildings." Dissertation Paper for Ph.D., University of California at Berkeley, 1991.